I. Introduction

Atmospheric optical phenomena result from visible light interacting with the earth's atmosphere and aerosols. While studying such phenomena has some practical use to scientists, most of society's relationship with atmospheric optics is simply the enjoyment of a rainbow after a passing storm or watching a fiery red sunset in the western sky. As rays of light pass through the atmosphere, they interact with the atmosphere, causing the rays to change their path to the earth's surface. When light hits an interface of two media of different densities, the light can either reflect off the surface or penetrate and refract. Refraction causes light rays to bend when they encounter media of different densities. Reflections can produce sun pillars, and are an important aspect of rainbows. These phenomena can all be seen with the naked eye, but the important interactions occur on very small scales. This paper will examine several types of optical phenomena in the atmosphere, as well as some of the governing principles of optics.

II. Refraction

To get a basis of understanding for refraction, it is necessary to understand the behavior of light when it passes between media. Light traveling through material travels at a speed less than the speed of light in a vacuum. The non-dimensional refractive index is the factor by which the speed of light through the medium needs to be increased to be equivalent to the speed of light. The index of refraction, n, is mathematically defined as:

$$n = c / v \qquad \text{.....(1)}$$

where c is the speed of light in a vacuum and v is the velocity of light in the medium. When considering dry air, the first order approximation for the index of refraction is given by

$$(n-1) = a(\lambda)\rho_d \qquad \text{.....(2)}$$

in which ρ_d is the density of dry air as a function of pressure and temperature and the empirical parameter, *a*, which has a wavelength dependence across the entire electromagnetic spectrum. The value of *a* in the visible band is approximately constant at 2.34×10^{-3} m^3/kg, resulting in an *n* value near 1.0003 at the earth's surface. The dependence of the index of refraction on density will play an important role in mirages, because *n* decreases with height.

A wave front traveling through a medium with a constant index of refraction will travel in a straight line. If, however, the wave encounters a boundary between different *n* values, the transmitted wave will refract because the wave speed will change. If the wave passes into a faster medium ($n_2<n_1$), the direction of the wave will refract away from the line perpendicular to the boundary. Conversely, if the wave passes to a slower medium ($n_2>n_1$), the direction of the wave will refract towards the line perpendicular to the boundary. If the wave hits perpendicular to the boundary, there is no bending of the wave. This relationship can be mathematically explained using Snell's Law. Consider the wave front in Figure 1 as it crosses an interface of lower to higher *n* value. Over the time period, Δt, the wave travels L_1 and L_2 in media I and II respectively. With $L_1 = v_1 \Delta t$, velocity and distance traveled can be related by $L_1/L_2 = v_1/v_2$. Using equation (1) and $L_1 = AB\sin(i)$ and $L_2 = AB\sin(r)$, Snell's Law can be shown

$$\frac{n_2}{n_1} = \frac{\sin(i)}{\sin(r)} \qquad \text{.....(3)}$$

where *i* is the angle of incidence and *r* is the angle of refraction, both measured in relation to the line normal to the boundary. This equation is fundamental in understanding nearly all atmospheric optical phenomena. Note in Figure 1 that on observer perceives the light

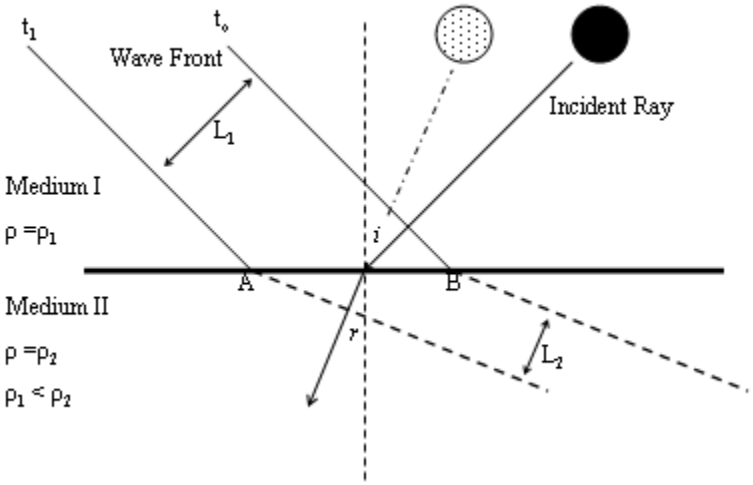

Figure 1 - The incoming ray from the black circle hit the interface at angle *i* and refracts at angle *r*. An observer sees the apparent position of the circle as the hashed circle to the left

source away from its true location. This phenomenon is easily seen in real life when you stick a straw into water and the straw appears bent.

In a situation with parallel layers of media with different values of *n*, the angle of refraction is only dependent on the initial angle of incidence and the initial and final n values. Figure 2 demonstrates the simple cases where a ray enters then exits a layer of more optically dense material. The final direction of the ray is parallel to the incident ray. However if the surface interfaces are not parallel, the resulting ray does not travel in the same direction as the initial ray.

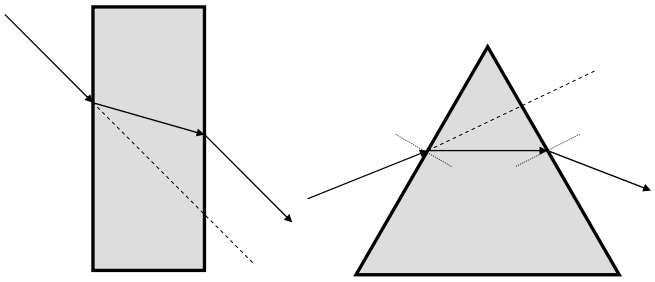

Figure 2 - When the prism surfaces are parallel such as on the left, the exiting ray is parallel to the incidence ray. On the right the prism surfaces aren't parallel and the exiting ray is not parallel to the incident ray.

III. Rainbows

Applying Snell's Law to spherical water drops results in the theory of the formation of rainbows. As light traveling through air hits the surface of the water droplet,

some light is reflected off the surface (Fig. 3.a), while the rest travels through the water. Upon reaching the other side of the droplet, some light travels through boundary (3.b), and some is reflected internal to the drop (3.c). It is this reflected light that is responsible for creating rainbows. Prior to the formulation of Snell's Law in 1621, Antonia de Dominis showed rainbows could be formed by light hitting the water drop being refracted, reflected, then refracted again (Stevens, 1906). After Snell's discovery, Descartes applied it to the rainbow problem, discovering a geometric solution. Descartes hypothesized that color was a product of refraction. It was later shown by Isaac Newton, that each wavelength of light has a unique index of refraction. In water, the differences of the index of refraction are not negligible across the visible light spectrum.

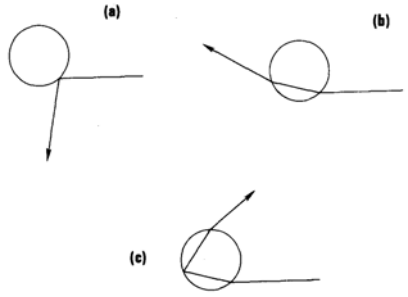

Figure 3 - Possible paths of incoming rays when encountering a water drop (Walker, 1975)

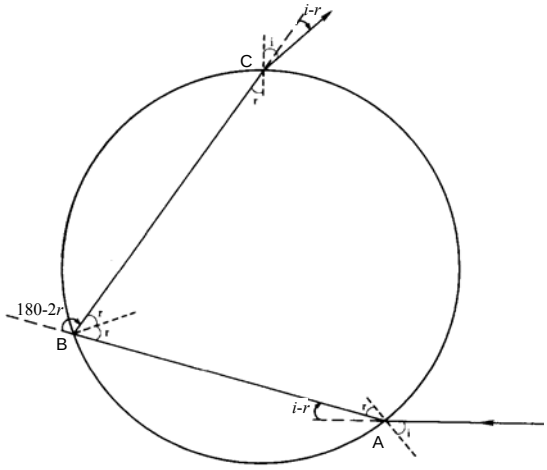

Figure 4 - The total deviation of the incident light ray is the sum of the deviations at points A, B, and C. The ray deviates (*i*-*r*) at A and C, while deviating 180^{o}-2*r* at B. Adapted from Walker.

The total deviation, *D*, of a light ray from its initial path can be calculated by tracing a ray over its path through the droplet (Fig 4). If the ray is subjected one reflection, then the total deviation from the initial direction is

$$D=180°+2i-4r \quad \ldots\ldots\ldots\ldots \quad (4)$$

in which *i* and *r* can be related by (3). Light rays hitting the droplet are assumed to be parallel because of how far the sun is from the earth. Figure 5 shows Descartes Theory for parallel rays hitting the raindrop. As the angle of

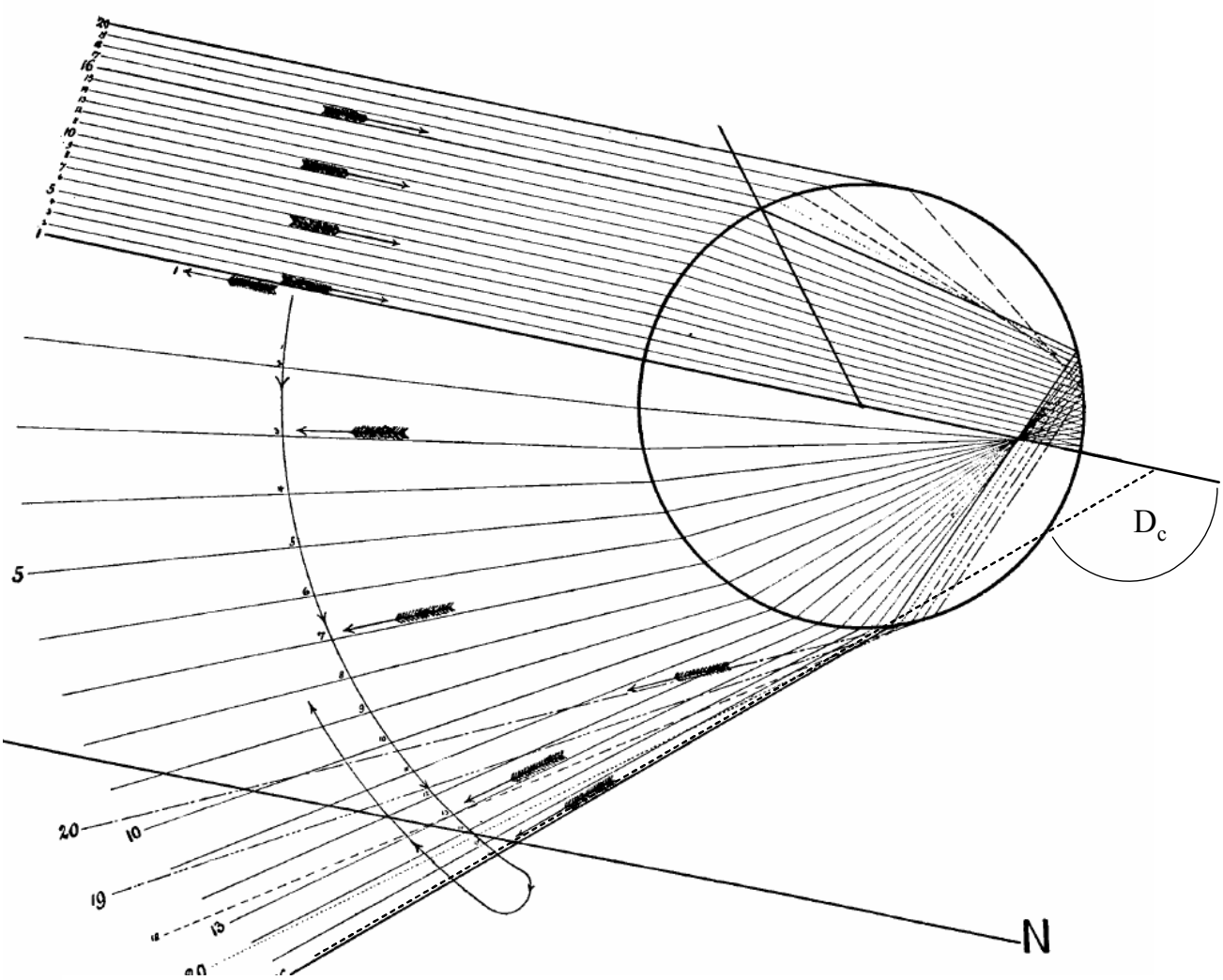

Figure 5 - Illustration of Descartes's theory of geometric refraction in a raindrop. Note the cluster of rays near the angle of minimum deviation. (Hammer)

incidence is increased as you get closer to the top of the droplet, the angle of refraction also increases. At a critical value, the deviation hits a minimum value. Close to this value, there is a bunching of rays. This higher density of rays corresponds with a more intense image for the viewer. Close to this limit, *D* has its smallest rate of variation, leading to more light accumulating at this angle (Hammer, 1903). It is due to this higher intensity of light that the observer can see a bow. *D* has a minimum at the point where *dD/di*=0. Taking the derivative of (4) with respect to *i* yields

$$\frac{dD}{di} = 1 - 2\frac{dr}{di} \qquad \text{.....(5)}$$

Where

$$\frac{dr}{di} = n_{H_2O}(\lambda)\frac{\cos(i)}{\cos(r)} \qquad \text{.....(6)}$$

Solving for the point where dD/di=0, results in

$$\cos(i) = \frac{\sqrt{(n^2-1)}}{3} \text{ and } \cos(r) = \frac{2}{n}\frac{\sqrt{(n^2-1)}}{3} \qquad \text{.....(7)}$$

Substituting these values for *i* and *r* into (4) produces the angle of minimum deviation, D_c.

Now let's add color. As mentioned above, the index of refraction is dependent on wavelength. In water, the differences of the index of refraction are not negligible across the visible light spectrum. This results in the white solar beam breaking up into different colors as it passes through the boundaries. Longer wavelengths, such as red in the visible spectrum, refract less than shorter wavelengths, such as blue. Based on this, it can be seen both in the equations and the sky that different colors have different values of minimum deviation, D_c. Table 1 displays the critical values of red and blue light. Colors that have a minimum value at D_c are then visible at angle of 180°-D_c above the direction parallel to the incoming rays. For the primary rainbow, 180°-D_c is equal to 42.3° and 40.6° for red and violet light respectively. Therefore, for a spectator on the ground, red appears at a higher angle of inclination than violet, meaning that red appears on the outer side of the bow.

Table 1 - The minimum deviation, D, for red and blue for the first 3 rainbows.

	D			*i*		*r*	
k	red	blue	*ΔD*	red	blue	red	blue
1	137.6	139.6	1.7	59.5	58.8	40.4	39.6
2	230.4	233.5	3.1	71.9	71.5	45.6	44.9
3	317.5	321.9	4.37	76.9	76.6	47	46.4

Supernumerary rainbows occur when there is more than one reflection occurring on the inner surface of the raindrop. Using the same logic, (4) and (7) for the general case with k internal reflections can be written as

$$D=180k+2[i-(k+1)r] \quad \text{.....(8)}$$

$$\cos(i)=\sqrt{\frac{n^2-1}{k^2+2k}} \quad \text{and} \quad \cos(r)=\frac{k+1}{n}\sqrt{\frac{n^2-1}{k^2+2k}} \quad \text{.....(9)}$$

With each reflection the incidence beam spreads more inside the drop, causing larger differences of D_c between red and blue light. The difference of these two values is the angular thickness of the rainbow (Table 1).

The secondary rainbow is produced by two internal reflections. The angle of minimum deviation for the secondary rainbow is near 232° (Fig. 6). For this rainbow, the red is on the inside of the bow, with violet on the outside. An observer can see a dark band between the primary and secondary bows. Raindrops between these bows cannot refract light to an observer on the ground, creating a dark band (Fig. 7).

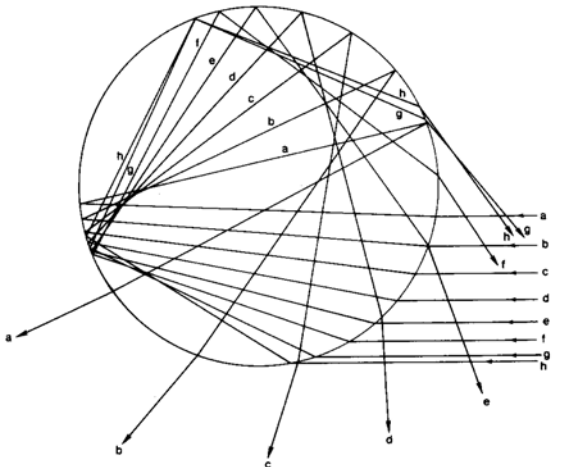

Figure 6 - Refraction from two internal reflections producing a secondary rainbow. (Walker)

In nature, only the first two rainbows are observed. (Walker, 1976) One reason that higher order rays are not seen is because i_c is closer to the edge of the drop, reducing the cross-sectional area receiving these rays. This causes a decrease in the intensity of these rays. Also, higher order rainbows are wider, meaning the dispersion of the rays will cause a weakening of observed intensity. A third reason for the decreased intensity of

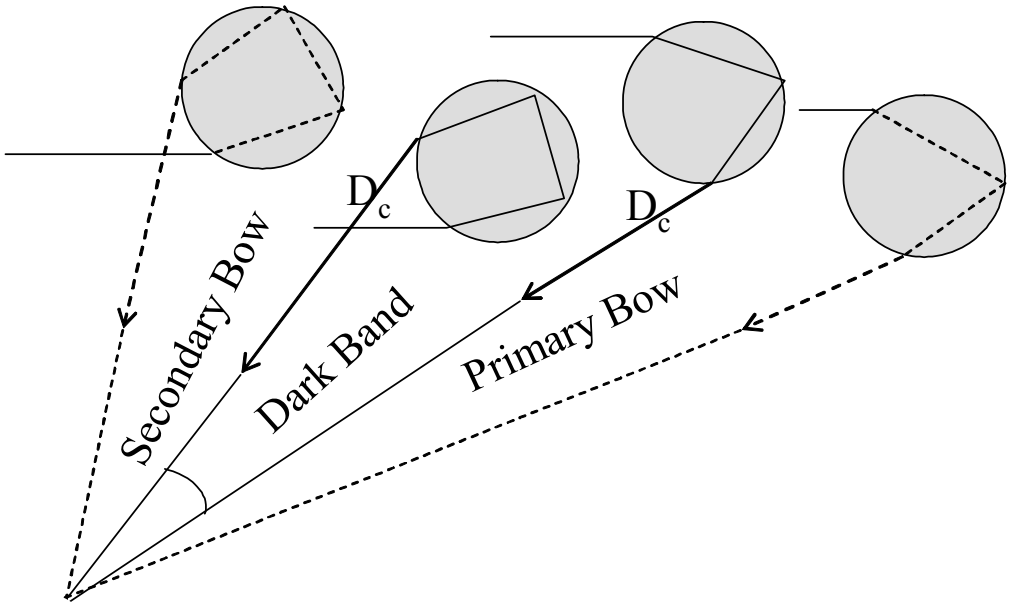

Figure 7 - Raindrops are incapable of refracting light within the dark band to the observer because it would require angles below D_c.

higher order waves is that at each reflection some light is transmitted through the edge of the droplet, so each subsequent has less intensity. Higher order rainbows cannot overcome the background radiation from clouds, raindrops, and scattering to be seen in nature.

So far, we have ignored diffraction, an effect that causes deviations from the geometric solutions of rainbows. The wave front entering the raindrop is altered by the time the leaves the drop (Hammer, 1904). This is an application of Huyghen's principle, where the propagating wave is the sum of waves propagating in concentric circles from each point. This creates an interference pattern such that some colors are enhanced or weakened from the perspective of the observer (Minnaert, 1954). The

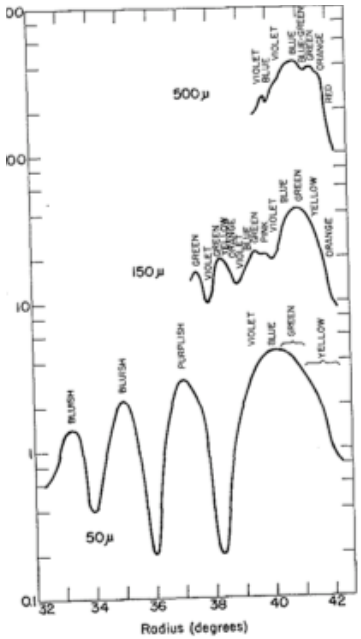

Figure 8 - Changes of intensity of the colors of the rainbow due to diffraction (Neuberger).

diffraction a phenomenon is a function of raindrop diameter, meaning a rainbow's color characteristics is determined by the size of the droplet. The size of the droplet can also cause a widening of the rainbow. Figure 7 shows the visible primary rainbow for three drop sizes (Neuberger).

II. Ice Phenomena

Other optical phenomena are observable by light interacting with ice crystals. The two most common ice crystals are hexagonal plates and hexagonal columns (Fig.9). Both types of crystals have refracting angles of 60°, when traveling through two sides spaced one face apart, and 90° when traveling through the top and out on of the sides. The orientation of the crystals relative to the incoming solar beam will determine which refracting angle is more likely. Typically column crystals are oriented with their principal axis horizontal. In this horizontal plane, they freely rotate around the vertical and principle axes, preferentially restricting it to two degrees of freedom (Woolard, 1936). Plate crystals are suspended in the atmosphere with their hexagonal surfaces horizontal to the ground, and tend to be restricted to one rotational axis about the vertical. These orientations, along with certain solar angles, produce various optical phenomena.

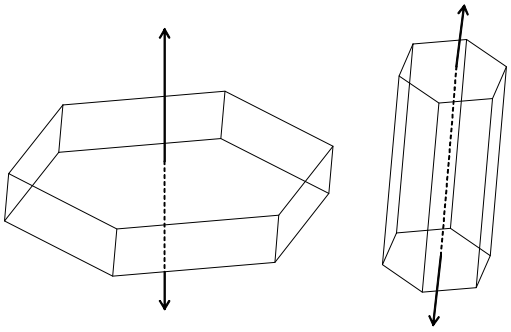

Figure 7 - The two basic shapes of ice crystals are the plate (left) and column (right) . The line denotes the principle axis.

Similar to the rainbow, ice optical phenomena occur at the angle of minimum deviation, because there is a concentrated beam that can be observed.. We can take the same approach for refraction through ice as through water drops. For simplicities sake,

we will consider rays that pass through the crystal without reflection. The total deviation from the incident beam is

$$D=(i-r)+(i'-r') \qquad \ldots\ldots\ldots\ldots(10)$$

which can be seen in Figure 10 .It can be shown geometrically that the refracting angle, A, can be described as $A=(r+r')$. Taking the first derivative of (10) and substituting in derivatives of Snell's Law results in

$$n=\frac{\sin\frac{1}{2}(A+D)}{\sin\frac{1}{2}A} \qquad \ldots\ldots\ldots\ldots(11)$$

where n is equal to the refractive index of ice (n=1.31). Therefore, for a refracting angle of 60°, D_c equals 22°. For the 90° case, D_c equals 45°.

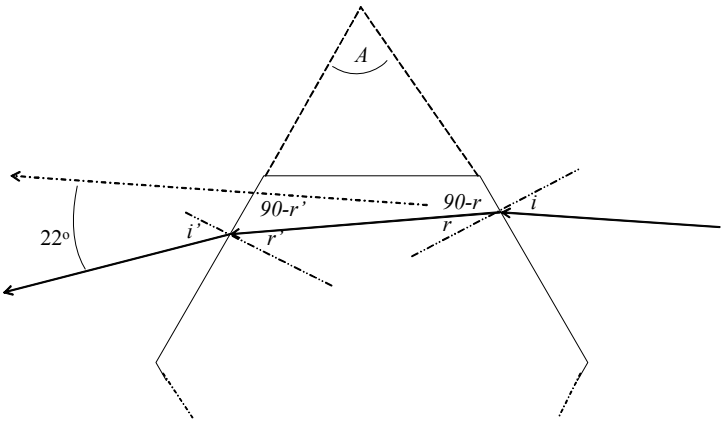

Figure 8 - For a refracting angle of A=60° the minimum deviation is 22°

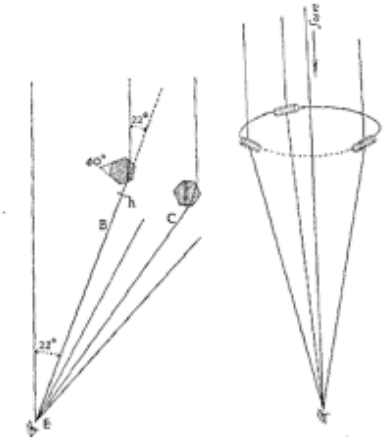

Figure 9 – Crystals with their principle axis horizontal produce a 22° ring around the sun. (From Minnaert)

One common phenomenon involves the column ice crystals when the sun is at a low zenith angle (high in the sky). Ice crystals associated with cirrus and cirrostratus clouds can form a layer of column-like ice crystals. Parallel beams of light coming from the sun are refracted as they pass through this layer. The result is a thin band of brightness that encircles the sun. Since the incident beam hits a side of the crystal, the refracting

angle 60°, resulting in an image at 22° (Fig. 10). Similar to the rainbow case, red light is refracted the least and is therefore at the inner edge of the ring. Colors follow the standard rainbow color scheme outward, however the spectrum is much less distinct in a halo. There is generally a crisp inner ring that occurs because of the angle of minimum deviation, but due to the random distribution of ice crystals, the halo color washes out. This is due to the fact that there are fewer incident rays on ice crystals that result in the minimum deviation, relative to the raindrops of a rainbow (Tricker, 1970). The rays for minimum deviation to occur must be perpendicular to the principal axis and strike that surface at the exact critical incident angle. With fewer rays that cause the desired optical image, there are more rays that cause this image to be less intense. Halos can also be visible at night as a pale ring around the moon. When the crystals deviate from their horizontal alignment, it is possible for the 90° refracting angle to create a 45° halo. This rarer halo also has red on the inner side, and similarly washes out color as you move towards the outer bands.

The other most common phenomena involving ice crystals are parhelia, also known as sundogs. These parhelia appear as bright spots of light on either side of the sun at high zenith angles (low over horizon). Parhelia are result of thin plate-like ice crystals fluttering with the principal axis vertical. The refracting angle A=60° creates these phenomena. They appear to be red at the innermost point, and fade to indistinct colors after that, for similar reasons to the halo (Tape, 1990). Parhelia aren't visible exactly at the 22° as predicted by (11). Instead, rays that hit the ice crystal are skewed because the incident ray is not perpendicular to the principal axis of the ice crystal. In this case, the angle of minimum deviation D' is a function of the sun's elevation, h

$$\frac{\sin\frac{1}{2}(A+D')}{\sin\frac{1}{2}A}=\sqrt{\frac{n^2-\sin^2 h}{1-\sin^2 h}} \qquad \text{.....(12)}$$

At higher sun elevations, the parhelia occur at greater angles from the sun (Tricker, 1970).

Not all optical phenomena involving water require refraction. In the case of sun pillars, reflections off the ice crystal surfaces produce a tall bright column appearing above the sun. In order for this phenomenon to occur, the sun has to be at an elevation angle less than 15° above the horizon. Sun pillars require hexagonal plate crystals or broken fragments of snowflakes (Currie, 1935). As the ice crystals flutter with their principal axis vertical, small deviations from this position will reflect light from the sun to the observer (Fig. 12). This small tilting produces a narrow column of light centered over the sun. Since there is no refraction occurring, the incident ray of sunlight is not split into separate colors, therefore the color of the sun pillar is the same as the light source.

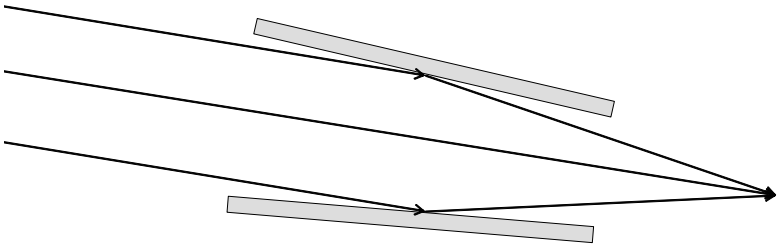

Figure 10 - Parallel light reflecting of f of the surfaces of ice crystals creates the appearance of a pillar of light located above the sun.

IV. Atmospheric Refraction

When the light rays from the sun travel through the earth's atmosphere, their paths do not follow straight lines. Density in the earth's atmosphere is not constant with height, and since the refractive index of air is density dependent, as seen in (2), the light ray will refract (Pernter, 1910). By taking the vertical derivative of (2) and applying geometry, it

can be found that *dn/dz* and the radius of curvature, *r*, is a function of temperature lapse rate.

$$\frac{dn}{dz} = -\frac{(n-1)}{T}\left[\gamma_h - \gamma\right] \qquad \text{.....(13)}$$

$$\frac{1}{r} = \frac{(n-1)}{nT}\left[\gamma_h - \gamma\right] \qquad \text{.....(14)}$$

The homogeneous lapse rate, $\gamma_h = g/R_d$, is the temperature profile necessary to achieve constant density in a layer. At this lapse rate, rays travel in straight lines. Although n is a function of wavelength, differences of n between colors in the visible spectrum is very small and (in most cases) is negligible. Light rays appear to bend toward higher densities, therefore in normal atmospheric conditions ($\gamma < \gamma_h$) light rays bend towards earth ($r > 0$). In the cases of very high temperature lapse rates ($\gamma > \gamma_h$), density decreases with height and light rays bend upward ($r < 0$). These differences in lapse rates are the basis for mirages, when objects appear as being displaced and distorted from their true position.

The best way to visualize mirages with pen and paper is by ray tracing. By tracing the path of a ray from an object to an observer, it is possible to determine where the image appears to the observer. In the case of strongly stably stratified air ($\gamma << \gamma_h$) a ray traveling from the object at an upward angle from the horizontal will be refracted downward with radius (+)*r*. For the observer, this ray will be hitting their eye at a downward angle, making the object appear above its true position. This is known as a *looming* mirage. This phenomenon often occurs over cold northern waters. Warm air from land is advected over the cold ocean, setting up conditions for a looming mirage, and making distant islands or ships appear to be above the horizon.

In a case of a very large temperature lapse rate, air at the surface is relatively less

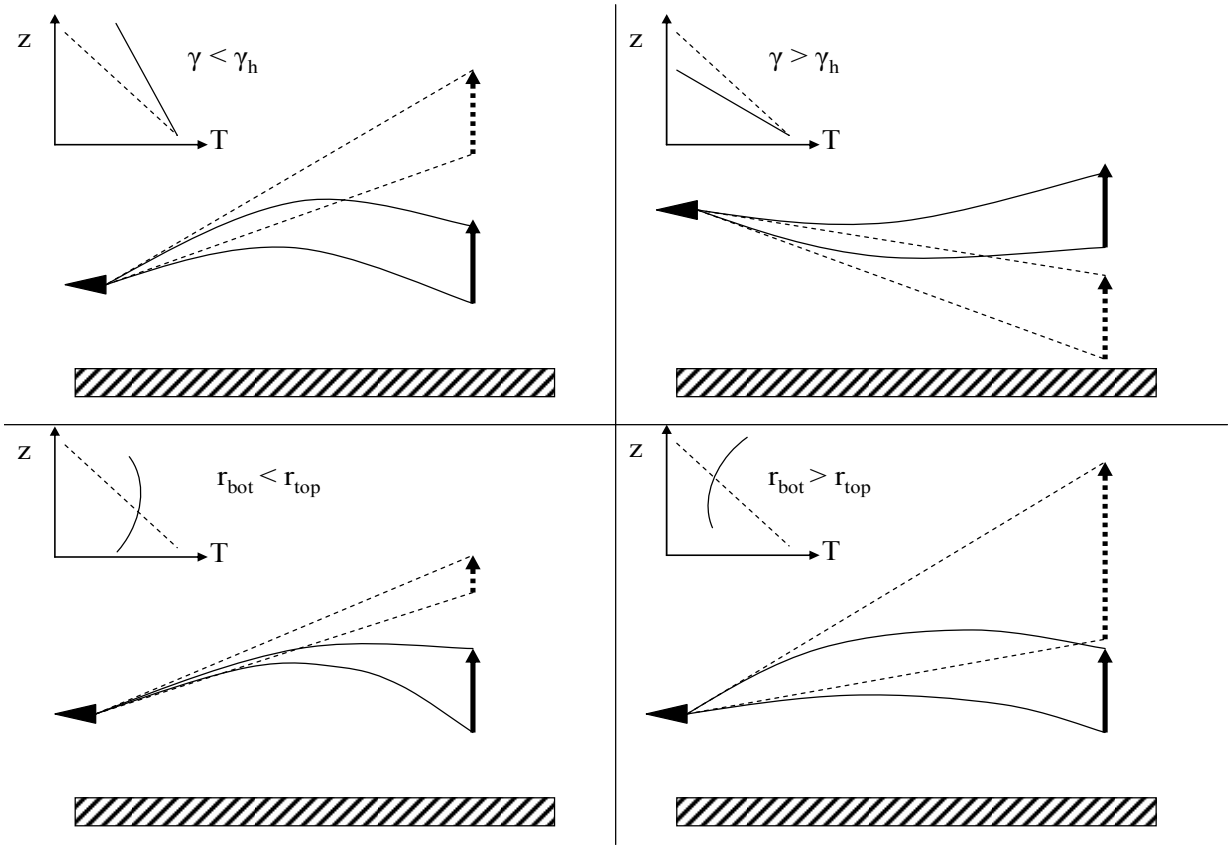

Figure 11 - Various effects of different temperature lapse rates. The dashed line in the inset pane represents the homogeneous lapse rate. The image that the observer views is the dashed arrow.

dense and results in the ray having a negative radius of curvature. For the observer, rays coming from the object will appear at a downward angle, resulting in a *sinking* mirage. Most drivers are familiar with this phenomenon when on bright sunny days they see what appear to be puddles in the road. The black asphalt absorbs solar radiation and conducts this heat to the air at the surface. Light coming from the distance is refracted back up to the viewer. Due to the non-uniformity of the temperature gradient, the driver sees a rippled mirage of the sky or trees in the distance. Large changes of the lapse rate with height can have a distorting effect, causing the image to stretch or shrink. This is a result of the effective rays at the top of the object having different radii of curvature from rays at the bottom, causing them to appear to be stretched or shrunk. In some extreme cases,

the shrinking is so extreme that the image flips. Figure 13 depicts several ray diagrams of different lapse rate scenarios and the images they would produce.

Since under most atmospheric conditions density decreases with height, there is usually some downward curving of rays. This means that the apparent horizon is farther away than the geometrical horizon. The apparent horizon is located at a distance, *d*, from the observer standing at elevation *H*.

$$d = \sqrt{\frac{r}{r-H}}\sqrt{2RH} \qquad \text{.....(15)}$$

where R is the radius of earth, and the radius of curvature can be found using (14). In the case that the lapse rate is the homogeneous lapse rate (r =0), the horizon is the geometric horizon, $d=(2RH)^{1/2}$.

It can be found using Snell's Law that the greatest change in angle of refraction occurs when the incident angel is nearly tangent to the prism surface. In the atmosphere, this is analogous to when the sun is at very high zenith angles (close to the horizon). This increased refraction has several consequences when the sun is either rising or setting. First, the sun is still viewable even after the sun has set over the geometric horizon. This also occurs prior to sunrise. Sometimes when the sun is just below the apparent horizon, there is a small bright spot of bluish-green light occurring just above the sun. At these low sun angles, a lot of the orange, yellow, and some red light is absorbed by water vapor, leaving mostly red and blue/green light reaching the observer (Pernter, 1910). The *green flash* is a result of increased refractivity of shorter wavelengths, such that for an observer looking at the setting sun, the increased bending of green light can be the only color seen when the sun is just below the horizon. The intensity of the green light is small compared to the rest of the solar disk, so it is necessary for the sun to be out of

view on order to see the green flash. Due to the necessity for zenith angles near 90°, green flashes are predominately observed over long fetches of water.

V. Absorption and Scattering

The way light interacts with aerosols and gases depends on the composition and size of the scatterer in comparison to the wavelength of light. Absorption of light depends on the scatterer and the incident wavelengths. Water vapor and carbon dioxide selectively absorb wavelengths near the infrared. In the stratosphere, ozone is a very effective absorber of ultra-violet light. The reemission of heat from ozone molecules warms the stratosphere, creating the tropopause and a temperature maximum near 45km (Gowan, 1931). There is not much absorption of light in the visible spectrum by the atmosphere, other than some of yellow to orange light by water vapor. This allows us to see all colors at great distances.

An incoming ray of light has a certain frequency which can be related to the wavelength. There is also an associated electrical field inherent in electromagnetic radiation. As a wave of electromagnetic passes a particle, the electric field excites oscillations of dipolar molecules at the same frequency as the incident wave (van de Hulst, 1957). The molecule then creates its own radiation in all directions, at the same frequency, and therefore color of the incident wave. These interactions cause a weakening of intensity of the incident light, while causing observable radiation in all directions. This is the basic, fundamental principle of scattering.

When particles are small relative to the wavelength, Rayleigh scattering occurs. For the visible spectrum, individual gas particles act as scatterers (Rayleigh, 1918). The strength of Rayleigh scattering is a function of the wavelength and refractive index of the

incident radiation. Beer's Law relates scattered irradiance to a path length proportional to a scattering coefficient

$$\frac{dE}{E} = -k_s dz \qquad \text{.....(16)}$$

where

$$k_s = \frac{8}{3}\frac{\pi^3}{N_o \lambda^4}\left(n_o^2 - 1\right)^2 \qquad \text{.....(17)}$$

assuming the scatterers are isotropic spheres with a number density of N_o. The most significant thing to note from (17) is the strong inverse dependence on wavelength to the forth power. This means that in the atmosphere, shorter wavelengths scattered more. The most apparent result of this phenomenon is the blue sky. Scattered light from the intense solar beam consists primarily of blue light, while longer wavelengths, such as red, are constricted more to the solar beam. Therefore, away from the sun, the diffuse downward radiation appears blue. When the sun is near the horizon, the optical path through the atmosphere is much longer, nearly all of the blue light is scattered from around the solar beam and more red is in the light that appears around the sun. This causes the some of the redness associated with sunrises and sunsets.

Mie scattering occurs when the scatterers are larger compared to the wavelength. Atmospheric aerosols from dust and pollution are primarily responsible for this type of scattering. As opposed to Raleigh scattering, most of Mie scattering is in the same direction as the incident light. There is also a smaller dependence on wavelength. Thus on hazy or polluted days the sky appears gray because all wavelengths are being scattered toward the surface nearly equally (Houghton, 1985).

VI. Concluding Remarks

Most of what is known about atmospheric optics has been known and well understood for over 300 years. The basic refraction principles of Snell and Descartes from the 17th century are still valid today. Near the turn of the 20th century, there was a newfound interest in studying some of these phenomena. A more thorough understanding of diffraction was found, as well as better measuring of atmospheric conditions during optical events. Current research deeper into the study of atmospheric phenomena is somewhat impractical. A quick search for papers on optics, rainbows, and halos in the past 30 years yields very little. There are very few current secrets of these atmospheric phenomena, and the secrets that are still unsolved are not essential to understand.

This paper aimed to give scientific explanations of a variety of these optical phenomena. Nonetheless, it is not necessary to have any bit of scientific understanding to enjoy and appreciate them. Children are wishful that they will one day find the pot of gold at the end of a rainbow. Farmers used to take the halo as a sign of rain in the next 24 hours, as the high cirrus clouds moved in ahead of an approaching front. A sailor who sees the green flash will never err again in the matter of love. These romanticized ideas surrounding optical phenomena will leave people looking toward the sky in the hopes of seeing something spectacular.

References

Aguardo, E. and J. Burt, 2004. *Understanding Weather and Climate* (Pearson, New Jersey).

Curie, B., 1935. Ice crystals and halo phenomena. *Monthly Weather Review*, Feb., 57-58.

Gowan, E., 1931. Effect of ozone on temperature of the upper air. *Monthly Weather Review,* Feb., 80-81.

Hammer, D., 1904. Airy's Theory of the rainbow. *Monthly Weather Review*, Nov., 503-508.

Houghton, H., 1985. *Physical Meteorology* (MIT Press, Cambridge).

Minnaert, M., 1954. *The Nature of Light & Color in the Open Air* (Dover, New York).

Neuberger, H., 1951. *Introduction to Physical Meteorology* (Penn State, University Park).

Pernter, J., 1910. *Meteorologische Optik*. (Braumuller, Vienna).

Rayleigh, 1871. On the scattering of light by small particles. *Phil.Mag.*, 39, 447-454.

Sodha, M. et al, 1967. Image formation by optically stratified medium: optics of mirage and looming. *Brit. J. Appl. Phys*, 18, 503-511.

Stevens, W., 1906. Theory of the rainbow. *Monthly Weather Review*, Apr., 170-173.

Tape, W., 1994. *Atmospheric Halos* (American Geophysical Union, Washington).

Tricker, R., 1970. *Introduction to Meteorological Optics* (Elsvier, New York).

Van de Hulst, H., 1957. *Light Scattering by Small Particles* (Wiley, New York).

Walker, J., 1975. Multiple rainbows from single drops of water and other liquid. Amer. J. of Physics, 5, 421-433.

Woolard, E., 1936. The geometrical theory of halos. *Monthly Weather Review*, Oct., 321-325.